Finite-amplitude steady waves in plane viscous shear flows

By F. A. MILINAZZO† AND P. G. SAFFMAN

Applied Mathematics, California Institute of Technology, Pasadena, CA 91125

Computations of two-dimensional solutions of the Navier–Stokes equations are carried out for finite-amplitude waves on steady unidirectional flow. Several cases are considered. The numerical method employs pseudospectral techniques in the streamwise direction and finite differences on a stretched grid in the transverse direction, with matching to asymptotic solutions when unbounded. Earlier results for Poiseuille flow in a channel are re-obtained, except that attention is drawn to the dependence of the minimum Reynolds number on the physical constraint of constant flux or constant pressure gradient. Attempts to calculate waves in Couette flow by continuation in the velocity of a channel wall fail. The asymptotic suction boundary layer is shown to possess finite-amplitude waves at Reynolds numbers orders of magnitude less than the critical Reynolds number for linear instability. Waves in the Blasius boundary layer and unsteady Rayleigh profile are calculated by employing the artifice of adding a body force to cancel the spatial or temporal growth. The results are verified by comparison with perturbation analysis in the vicinity of the linear-instability critical Reynolds numbers.

1. Introduction

The study of finite-amplitude steady waves in a viscous fluid moving in shear flow at moderate to high Reynolds number is currently a subject of some interest, and a significant number of papers have appeared in recent years. There appear to be two main reasons for the studies. First, the waves provide a nice example of bifurcation in flows of some physical relevance, and, secondly, it is hoped that their existence and stability may throw light on the mechanism of transition to turbulence, especially when the bifurcation is subcritical and the experimental transition occurs at Reynolds numbers somewhat lower than the critical Reynolds number for linear instability. For instance, a claim that the onset of turbulence in plane channel flows at Reynolds numbers well below the critical value for linear instability can be explained by the three-dimensional instability of two-dimensional quasi-equilibrium states has been made by Orszag & Patera (1983). It has also been suggested tentatively (Saffman 1983) that finite-amplitude steady waves are simple members of a class of vortical states whose three-dimensional features may model properties of fully developed turbulence and that the physical existence of turbulent flows depends upon the mathematical existence of the vortical states. This point of view appears to have independently motivated unsteady calculations by Rozhdestvensky & Simakin (1984), whose three-dimensional secondary flows have profiles remarkably like those of turbulent flow. Also, Goldshtik, Lifshits & Shtern (1983) have calculated

† Present address: Royal Roads Military College, Victoria, B.C., Canada.

three-dimensional vortical states in Poiseuille flow and have found that these exist at somewhat smaller Reynolds numbers corresponding to the onset of turbulence.

Analytical and perturbation methods are powerful and informative techniques for questions of existence, but their quantitative content is limited to waves of small amplitude, for which the alteration of the basic uniform laminar state is small. For the study of waves of finite amplitude and their properties, particularly their stability to three-dimensional disturbances, numerical methods appear more useful, although they are not, of course, without their problems and uncertainties. In the present paper we intend to describe the results of a numerical investigation of the finite-amplitude shear waves that can exist in a number of flows, motivated by the following reasons.

(i) Most of the studies of viscous finite-amplitude waves have been carried out for plane Poiseuille channel flow. Herbert (1981) reviews this work. (A general discussion of such an approach was given by Noether (1921).) It is now well established that finite-amplitude two-dimensional steady waves exist in plane Poiseuille flow for Reynolds numbers greater than a minimum which is about half the value for linear instability. However, the published calculations on steady states in plane Poiseuille flow employ almost entirely a Galerkin-type method with only two modes in the streamwise direction, the exception being that of Herbert (1978), who checked in some cases with three and four modes. The justification for this is that the contribution to the energy from the second mode is very small. It was therefore thought desirable to check the results by a different method that allows easily (although not necessarily cheaply) the inclusion of more modes. The results do not appear to be significantly different, but more detail is obtained about the minimum Reynolds number for finite-amplitude waves to exist. It also seemed worth investigating the fact that the minimum Reynolds number based on flow rate may differ somewhat from that based on average pressure gradient.

(ii) There is controversy over the existence of finite-amplitude waves for Couette flow, since this flow is stable for infinitesimal disturbances, and the existence of finite-amplitude waves implies a bifurcation from infinity. We hoped to carry out and report on a systematic search for such waves and examine the properties of finite-amplitude waves in Poiseuille–Couette flow. It is relevant that recently Smith & Bodonyi (1982) demonstrated analytically a bifurcation from infinity in Poiseuille flow through a circular pipe, which also has no neutrally stable finite Reynolds number. The discovery of finite-amplitude waves in plane Couette flow would suggest as a good possibility that these waves exist in circular Poiseuille flow at finite Reynolds numbers.

(iii) There are other flows to which the same methods apply that have physical interest. One example is the suction boundary layer on a flat plate. Experimental evidence on transition in this flow will provide another means of testing the hypothesis that the existence and stability of finite-amplitude waves are related to transition and the occurrence of turbulence.

(iv) The problem of finite-amplitude waves in boundary layers, wakes, jets and similar spatially developing flows are currently intractable by the present methods, which assume that the disturbances are spatially periodic. Various artifices have been employed in attempts to circumvent this problem. We wished to investigate the consequences of an approach (which seems to be due originally to Prandtl†) in which the growth of the boundary layer etc. is suppressed by the addition of a fictitious force that makes the parallel flow with the appropriate velocity profile, say the Blasius profile or the Rayleigh profile, an exact solution of the Navier–Stokes

† The idea is 'well-known', but we are unable to locate the precise reference.

equations. The problem is then formally well defined, and the methods can be applied and the results compared with experiment. However, the approach is intuitive rather than rational, and its value depends more on the insights that it provides into the sensitivity of the finite-amplitude waves to the undisturbed velocity profiles than on the detailed quantitative predictions.

2. Plane Poiseuille–Couette flow

We consider two-dimensional flow of a viscous liquid in a channel of width $2h$ ($-h < y < h$). It is assumed that the flow is steady in a coordinate frame moving parallel to the walls with speed c and periodic in the streamwise direction with a wavelength L. Thus we search for solutions of the Navier–Stokes equations in which the stream function Ψ, with $u = \Psi_y$, $v = -\Psi_x$, has the form

$$\Psi = \Psi(x-ct, y) = \Psi(x-ct+L, y), \tag{2.1}$$

which satisfies

$$(\Psi_y - c)\,\nabla^2\Psi_x - \Psi_x\,\nabla^2\Psi_y - \nu\,\nabla^4\Psi = 0, \tag{2.2}$$

where ν is the kinematic viscosity. The boundary conditions are

$$\Psi(x, -h) = 0, \quad \Psi_y(x, -h) = 0, \quad \Psi(x, h) = Q, \quad \Psi_y(x, h) = V, \tag{2.3}$$

where Q is the total flux through the channel and V is the velocity on the top wall. The bottom wall is supposed at rest. In general, a pressure gradient will be necessary to drive the flow and the average kinematic pressure gradient, $-P$ say, will be given by

$$P = \frac{-\nu}{2h}[\overline{\Psi_{yy}}]^h_{-h} = -\nu\,\overline{\Psi_{yyy}} + \frac{\mathrm{d}}{\mathrm{d}y}\,\overline{uv}, \tag{2.4}$$

where the overbar denotes an average over the wavelength L, and P is positive in Poiseuille flow.

Three physical Reynolds numbers can be defined for this flow configuration. They are

$$R_Q = \frac{3Q}{4\nu}, \quad R_P = \frac{h^3P}{2\nu^2}, \quad R_V = \frac{Vh}{\nu}. \tag{2.5}$$

The constants are chosen so that the first two are equal to $U_0 h/\nu$ in the case of uniform (i.e. independent of x) Poiseuille flow with centreline velocity U_0 and stream function

$$\Psi = U_0 h\left(\frac{2}{3} + \frac{y}{h} - \frac{y^3}{3h^3}\right). \tag{2.6}$$

Poiseuille flow is obviously defined by $V = 0$, irrespective of whether the flow is uniform. On the other hand, non-uniform Couette flow is not unambiguously defined. For definiteness, we shall define it by the condition $P = 0$, which seems physically to make most sense. The steady states of the system are therefore described by a surface in the four-dimensional space with coordinates $(R_P, R_Q, R_V, h/L)$. The intersection with the plane $V = 0$ gives Poiseuille flow, and the intersection with the plane $P = 0$ gives Couette flow.

It is clear that, for given values of h/L, any two of P, Q, or V may be chosen independently. The uniform solution for Poiseuille–Couette flow is

$$\Psi = Vh\left(\frac{1}{4} + \frac{y}{2h} + \frac{y^2}{4h^2}\right) + \tfrac{3}{4}(Q - Vh)\left(\frac{2}{3} + \frac{y}{h} - \frac{y^3}{3h^3}\right), \tag{2.7}$$
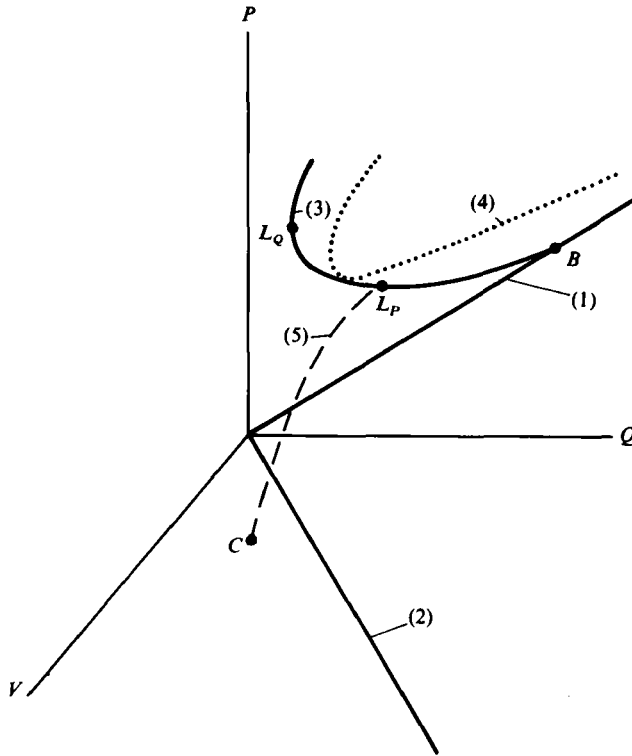
$$P = \frac{3\nu}{2h^3}(Q - Vh). \tag{2.8}$$

FIGURE 1. Configuration space for two-dimensional finite-amplitude waves in Poiseuille–Couette flow at fixed h and ν: (1) laminar Poiseuille flow; (2) laminar Couette flow; (3) envelope of finite-amplitude non-uniform waves in Poiseuille flow; point B, minimum-Reynolds-number bifurcation of Poiseuille flow, $R_Q = 5772$, $\alpha = 1.02$; point L_Q, state of minimum Q, $R_Q = 2493$, $\alpha = 1.38$; point L_P, state of minimum P, $R_P = 2920$, $\alpha = 1.33$; (4) a family of solutions for constant $\alpha > 1.12$ bifurcating from infinity or part of an isola; (5) speculative family of Poiseuille–Couette solutions with nonlinear Couette flow at C.

In this case the average centreline velocity is given by

$$U_0 = \frac{3Q}{4h} - \tfrac{1}{4}V. \tag{2.9}$$

The relations (2.8) and (2.9) will fail of course when the flow is non-uniform (i.e. x-dependent).

The object is to find non-uniform solutions of (2.2) subject to (2.3) and (2.4). It is important now to note that the problem as so far stated does not have isolated solutions and is degenerate, for, if $\Psi(x - ct, y)$ is a solution, then so is $\Psi(x - ct + \epsilon, y)$ for arbitrary ϵ. To obtain a family of isolated solutions and remove the degeneracy, some phase condition is required. This can be chosen in infinitely many ways. For convenience we used equations such as

$$\frac{\partial \Psi(0, 0)}{\partial x} = 0. \tag{2.10}$$

It must also be noted that the uniform flow is still degenerate since the wave speed c is undetermined in this case.

The formal procedure goes as follows; see also figure 1, where the approach is sketched in the (Q, V, P)-space. First, values of h, L and ν are chosen so that

$$\alpha = 2\pi h/L \qquad (2.11)$$

has a value such that a bifurcation point exists for uniform Poiseuille flow, i.e. there is a Reynolds number for which the profile is neutrally stable to disturbances of wavelength L. This is determined from the Orr–Sommerfeld equation and is a point in figure 1 lying in the plane $V = 0$ on the line given by (2.8). The family of non-uniform Poiseuille solutions emanating from this point with this value of α is found and followed by bifurcation and continuation procedures like those described by Keller (1977). In the first instance the continuation parameter is Q, and it is found that the bifurcation is subcritical, i.e. the locus of solutions in the (Q, P)-plane goes towards smaller Q, and that there exists a limit point past which the value of Q starts to increase. Continuation in the variable P was employed to get around the limit point, and continuation in the variable α, which is equivalent to changing L, is carried out to find families of solutions for other values of α, and to determine the envelope of the solution branches. This is shown in figure 1 by the solid curve (3), which starts at the point B corresponding to the minimum Reynolds number for transition in plane Poiseuille flow. The values of α vary along curve (3), increasing with the distance from B.

The envelope curve has a vertical tangent at L_Q where $Q = Q_L$. Non-uniform two-dimensional solutions do not exist if $Q < Q_L$, and this point gives the minimum Reynolds number, based on Q, for such solutions to exist. There is also a horizontal tangent at L_P where $P = P_L$, and solutions do not exist if $P < P_L$. Hence there is an alternative minimum Reynolds number based on P. These two Reynolds numbers are unequal, and moreover the wavelengths of the two solutions are different. The minimum values of R_Q and R_P are 2493 and 2920, and the values of α are approximately 1.38 and 1.33 respectively. (The Reynolds number of Herbert's calculations appears to be R_P, and his value of 2935 for a minimum critical number with $\alpha = 1.32$ agrees well when it is kept in mind that it is necessary to search in Reynolds number and α. We obtained the minimum by fitting a paraboloid to data in the neighbourhood of the minimum.) The value of R_Q where P is a minimum is 2678. The value of R_P where Q is a minimum is 3218. This raises the possibility (Saffman 1983) that the results of experiments or unsteady numerical simulations may depend upon the way the experiment is done or the calculation formulated. That is, an experiment or numerical simulation done with the flux kept constant may give different (unsteady) results from an experiment or simulation with the pressure gradient kept constant. This point was also made by Rozhdestvensky & Simakin (1984).

Another interesting feature is that the wavelength for the disturbance for lowest R_Q is not unstable for the Orr–Sommerfeld equation. For plane Poiseuille flow the maximum value of α for unstable disturbances is 1.11. Thus, for example, the branch of non-uniform solutions on which $\alpha = 1.32$ does not intersect the laminar branch given by (2.8), and is therefore either an isola or goes off to infinity, in which case there is a bifurcation from infinity. Attempts were made to determine which of these possibilities is the case, but resolution was lost as the Reynolds number increased. We did succeed, however, in continuing the lower part of the branch with $\alpha = 1.32$ up to $R_P = 10000$ without difficulty (with $N = 15$ and $M = 198$, see §3), and the indications are that non-uniform waves with short wavelengths are bifurcations from
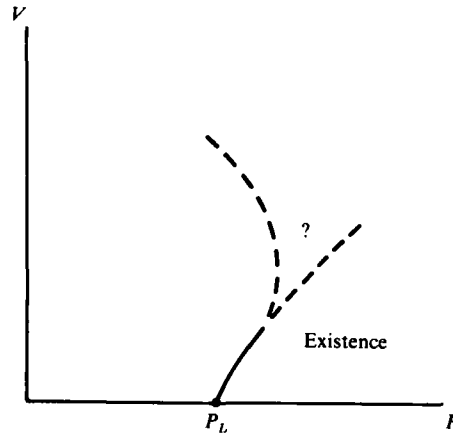
FIGURE 2. Boundary of configuration space for nonlinear waves in Poiseuille–Couette flow.

infinite Reynolds number. An illustration of a hypothetical family of solutions with constant α bifurcating from infinity is the dotted line (4) in figure 1.

To calculate waves in Poiseuille–Couette flow and search for waves in Couette flow, the procedure was to increase V (with h and ν fixed) for a non-uniform solution that allowed continuation in V, and then repeat the search as for Poiseuille flow to find the minimum value of P, P_L say, for the non-uniform solutions. This gives a curve in (P, V)-space that bounds the region where solutions exist. If P_L goes negative it means that solutions exist which are non-uniform Couette flows. If, on the other hand, P_L remains positive, then the implication would be that finite-amplitude non-uniform solutions do not exist in plane Couette flow. A sketch of preliminary results is shown in figure 2. The strange and unexpected result was found that P_L increased as V increased, at least for values of $R_V < 0.1 R_P$. This implies that two-dimensional vortical states do not exist for Couette flow. However, the computations were expensive, and the results are not definitive because only a limited range of V was explored. The possibility that the curve bends back as V increases further cannot be entirely ruled out, but the indications are that a search for three-dimensional states should be carried out.

The amplitude of the non-uniform solutions was measured by their kinetic energy per unit length

$$E = \frac{1}{2} \int_{-h}^{h} (\bar{u}^2 + \bar{v}^2) \, dy = E_0 + E', \tag{2.12}$$

where E_0 is the value for uniform flow:

$$E_0 = \frac{3Q^2}{10h} - \tfrac{1}{10}QV + \tfrac{2}{15}V^2 h. \tag{2.13}$$

3. Numerical methods

Calculations have been done for both channel flow and semi-infinite boundary-layer-type geometries. The numerical method for the former is a special case of the latter, and we shall therefore outline the numerical procedure just for the unbounded case, where (2.2) or a closely similar equation is assumed to hold for $0 < y < \infty$ and the wall is a no-slip streamline. The detailed implementation is straightforward but

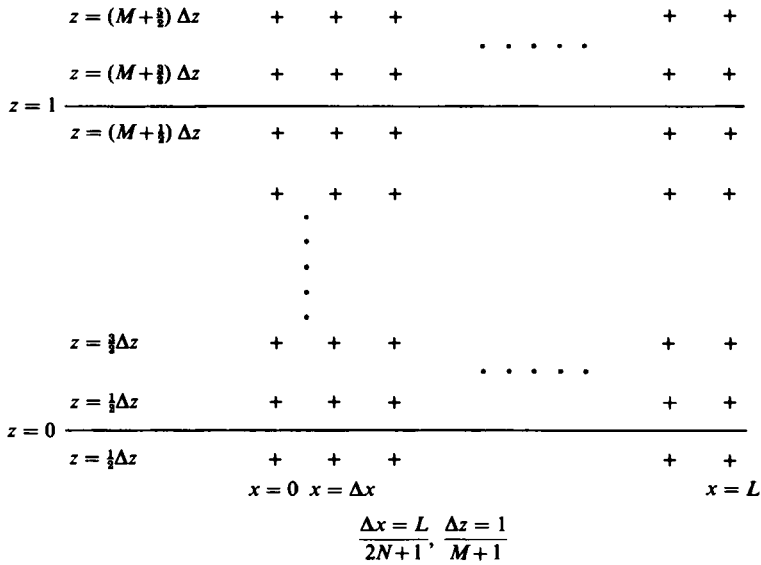$$\frac{\Delta x = L}{2N+1}, \quad \frac{\Delta z = 1}{M+1}$$

FIGURE 3. Computational mesh.

extremely involved. The partial differential equation is discretized by employing difference approximations for derivatives in y and pseudospectral approximations for derivatives in x. The analytic stretching

$$y = y_\infty \frac{e^{\beta z} - 1}{e^\beta - 1}, \tag{3.1}$$

is applied to the truncated interval $[0, y_\infty]$ in order to provide more resolution near the wall. Equation (2.2) is rewritten in terms of x and z, and the difference approximations are made on a grid with uniform spacing in x and z. Figure 3 shows the grid used for the computations. The computational points are at

$$\left.\begin{aligned} x_i &= i\,\delta x, \quad i = 0, 1, ..., 2N, \quad \delta x = \frac{L}{2N+1}, \\ z_{j+\frac{1}{2}} &= (j + \tfrac{1}{2})\,\delta z, \quad j = -1, 0, ..., M+2, \quad \delta z = \frac{1}{M+1}. \end{aligned}\right\} \tag{3.2}$$

Centred second-order-accurate approximations are made for the z-derivatives of Ψ at the points $j + \frac{1}{2}$ for $j = 1, ..., M$. The first and third and fourth derivatives involve five points. The x-derivatives are approximated using the pseudospectral method. For fixed j the values of Ψ at $i = 0, 1, ..., 2N$ are interpolated by a trigonometric polynomial of degree N. The result is differentiated and evaluated at the grid points to yield an approximation for the x-derivatives of Ψ.

The no-slip boundary condition yields the boundary conditions

$$\Psi_{i, -\frac{1}{2}} = \Psi_{i, \frac{1}{2}} = 0, \quad i = 0, 1, 2, ..., 2N. \tag{3.3}$$

Satisfying the discretized form of the differential equation at the grid points $i = 0, ..., 2N$, $j = 1, ..., M$ then gives $(2N+1)M$ equations. To obtain further equations it is necessary to match to the free stream.

For large y (2.2) reduces to the limiting form

$$\nu \nabla^4 \Psi - (U_\infty - c) \nabla^2 \Psi_x = 0, \tag{3.4}$$

where U_∞ is the constant free-stream velocity. Separating variables, it is seen that the y-dependence of the nth harmonic with wavenumber $n\alpha$ is

$$\Psi_n = A_n \, e^{\alpha_n y} + B_n \, e^{-\alpha_n y} + C_n \, e^{\beta_n y} + D_{\beta n} \, e^{-\beta_n y} \tag{3.5}$$

for $n \neq 0$, and

$$\Psi_0 = A_0 + B_0 y + C_0 y^2 + D_0 y^3, \tag{3.6}$$

for $n = 0$, where

$$\alpha_n = n\alpha, \quad \beta_n = \left[\alpha_n^2 + \frac{i\alpha_n}{n} (U_\infty - c) \right]^{\frac{1}{2}}, \tag{3.7}$$

and β_n is defined to have positive real part. Boundary conditions at $y = y_\infty$ that ensure that the solution matches to the decaying disturbance in the free stream are

$$\left. \begin{array}{c} (D^2 - \alpha_n^2) (D + \beta_n) \, \Psi_n = 0, \\ (D^2 - \beta_n^2) (D + \alpha_n) \, \Psi_n = 0, \end{array} \right\} \quad n = 1, 2, \ldots, N, \tag{3.8}$$

$$D^2 \Psi_0 = D^3 \Psi_0 = 0, \tag{3.9}$$

where $D \equiv d/dy$. Remembering that Ψ_n are complex for $n \neq 0$, these give $4N + 2$ real equations which are linear in the values of Ψ_{ij} for $i = 1, \ldots, N$ and $j = M - \frac{1}{2}, M + \frac{1}{2}, M + \frac{3}{2}, M + \frac{5}{2}$, when the z-derivatives are centred on $z = 1$. It is to be noted that B_0 is not put equal to U_∞, and we allow for a change in the free-stream velocity. This is a subtle point which we shall discuss further at a later stage. The value of A_0 corresponds to a change in the displacement thickness of the boundary layer.

At this stage the number of equations equals the number of unknown values of Ψ at the mesh points. We need one more equation because the wave speed is also unknown. This is provided by a phase condition, which also removes the spatial degeneracy of the formulation; a convenient one is to take the first derivative of Ψ to be zero for $i = 0$ and some j between 1 and M. The amplitude of the wave is not specified, since this comes out as a result of the calculation. For the case of flow in a channel, the boundary condition on the top wall specifies the values of Ψ for $j = M$ and $M + 1$, and the unknowns are the values for $1 \leqslant j \leqslant M - 1$ and the wave speed. The equation at the grid points and the phase condition gives the appropriate number of equations. The system of equations was solved by Newton iteration, with the first guess given either by continuation from a converged solution or from a solution of the Orr–Sommerfeld equation when the wave amplitude is small and the branch is near the bifurcation from the uniform flow.

4. Asymptotic suction profile

The flow field
$$u = U(1 - e^{-y/\delta}), \quad v = -W = \text{const.}, \quad \delta = \frac{\nu}{W} \tag{4.1}$$

is an exact solution of the Navier–Stokes equations and describes a constant-thickness boundary layer over a porous plate that is sucking in fluid with a constant velocity W. Finite-amplitude waves on this flow can be calculated as described in §3. There are two differences. First, there is an extra term $\nu \nabla^2 \Psi_y$ in the equation (2.2) for the
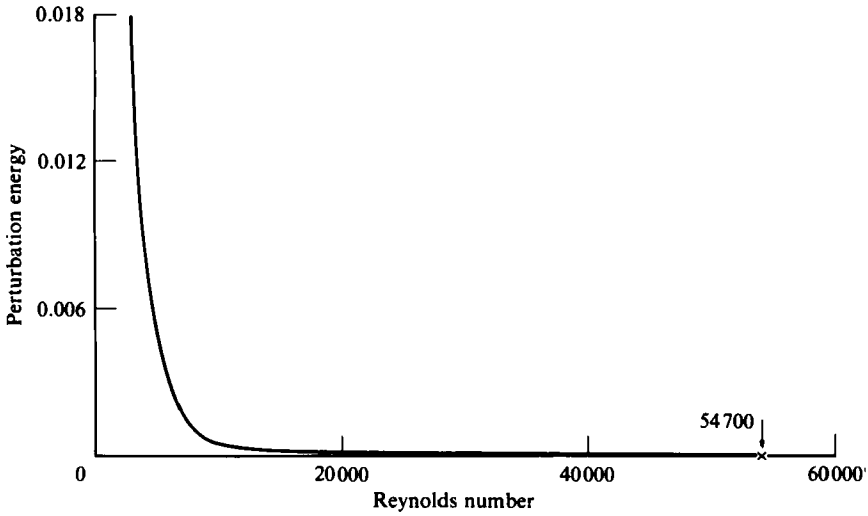
FIGURE 4. Asymptotic suction profile. Energy of disturbance normalized on $\frac{1}{2}U^2\delta$ versus Reynolds number $U\delta/\nu$. Boundary-layer thickness $\delta = \nu/W$. Results are for $\alpha = 0.16$, $N = 17$, $M = 149$, $y_\infty = 10$, $\beta = 5$.

stream function. Secondly, the boundary condition (3.9) is changed. Equation (3.6) is replaced by

$$\Psi_0 = A_0 + B_0\,y + C_0\,y^2 + D_0\,\mathrm{e}^{-y/\delta}. \tag{4.2}$$

We require $B_0 = U$ and $C_0 = 0$, which is achieved by imposing

$$\mathrm{D}^2\left(\mathrm{D}+\frac{1}{\delta}\right)\Psi_0 = 0, \quad \mathrm{D}\left(\mathrm{D}+\frac{1}{\delta}\right)\Psi_0 = \frac{U}{\delta}. \tag{4.3}$$

In this case the free-stream velocity is fixed. The counting is then as described in §3.

In figure 4 we show results of calculations of the wave amplitude, measured by its excess energy E', plotted against Reynolds number defined by

$$Re = \frac{U\delta}{\nu} = \frac{U}{W} \tag{4.4}$$

for $\alpha = 0.16$, where $\alpha = 2\pi\delta/L$. In this calculation δ and L were kept constant and ν was allowed to vary. The critical Reynolds number for instability of the laminar flow is about 55000 at this value of α (Hocking 1975; Drazin & Reid 1981). The data in the figure were obtained using $N = 17$, $M = 149$, $y_\infty = 10$ and the coordinate stretching parameter $\beta = 5$. The excess energy is normalized by $\frac{1}{2}U^2\delta$.

It is remarkable that the neutral curve drops so quickly to values of a few thousand from the large value for linear instability of the laminar profile. At a relative disturbance energy of 0.1 % the Reynolds number for existence of a steady non-uniform shear wave is 3000. According to the speculation by Saffman (1983), this would imply that the asymptotic suction boundary layer is unstable to very weak disturbances at Reynolds numbers an order of magnitude less than that predicted by linear stability theory, which is consistent with the general report that suction is not an effective way of laminarizing turbulent boundary layers, although it can delay transition.

5. Boundary layers

The results presented in §§2 and 4 are numerical approximations to exact solutions of the Navier–Stokes equations. It is natural to consider whether finite-amplitude shear waves exist in boundary layers on plates or bluff bodies. We are now faced with the fundamental difficulty that a boundary layer is only in exceptional cases (such as the asymptotic suction profile) independent of the streamwise coordinate x, say, because it is growing by the diffusion of vorticity, and the assumption of spatial periodicity (2.1) is not valid. In fact, the boundary layer or flow region must be treated as a whole, and both upstream and downstream boundary conditions need to be supplied for the elliptic equation (2.2). This is at present an insoluble problem, made even more difficult by the fact that the waves themselves must affect the boundary conditions, so that a boundary condition used in the absence of waves may be unreasonable when the waves are present.

In order to investigate finite-amplitude waves in boundary layers, *ad hoc* assumptions have to be made or physically unrealistic cases are studied. It is not our purpose here to consider the merits and demerits of the various approaches; rather we shall present results of calculations in which the boundary layer is modified by an artifice so that the flow field becomes amenable to the present technique. The extent to which the results bear on properties of real boundary layers is a matter for conjecture, but at least the approach has the merit of giving a well-posed problem, so it is clear exactly what problem is solved.

The artifice is to add a fictitious force in the x-direction so that the approximately unidirectional (or steady) velocity profile is an exact unidirectional steady solution of the Navier–Stokes equations on which a spatially periodic, steadily propagating wave can be superposed. We shall deal with two cases: the Blasius boundary layer and the Rayleigh profile. In the former the velocity profile given by the boundary-layer equations is

$$U = U_\infty f'\left(\frac{y}{\delta}\right), \quad V = \frac{U_\infty \delta}{2x}\left(\frac{yf'}{\delta} - f\right), \quad \delta = \left(\frac{\nu x}{U_\infty}\right)^{\frac{1}{2}}, \tag{5.1}$$

where

$$f''' + \tfrac{1}{2}ff'' = 0. \tag{5.2}$$

We replace the velocity field (5.1) by

$$U = U_\infty f'\left(\frac{y}{\delta_0}\right), \quad V = 0, \tag{5.3}$$

which is an exact solution of the Navier–Stokes equations if we add a fictitious force $-\nu U_\infty f'''(y/\delta_0)/\delta_0^2$ to the x-component of the momentum equation. Then, instead of (2.2), we calculate non-uniform solutions of

$$(\Psi_y - c)\nabla^2\Psi_x - \Psi_x \nabla^2\Psi_y - \nu \nabla^4\Psi = -\frac{K\nu\,U_\infty f''''}{\delta_0^3}. \tag{5.4}$$

Notice the variable K multiplying the force. The reason for its presence is that the force is not arbitrary, and there is no reason why the force can remain the same if non-uniform waves are present and all other parameters, e.g. the free-stream velocity or Reynolds number, are unaltered. The profile (5.3) solves (5.4) when $K = 1$, but when Ψ depends upon x we must allow K to change (or alter the profile in some other way). Referring back to (3.9) and the discussion of the way in which the boundary conditions at infinity are imposed, it was pointed out there that the counting did not allow for a specification of the free-stream velocity. The extra term on the right-hand
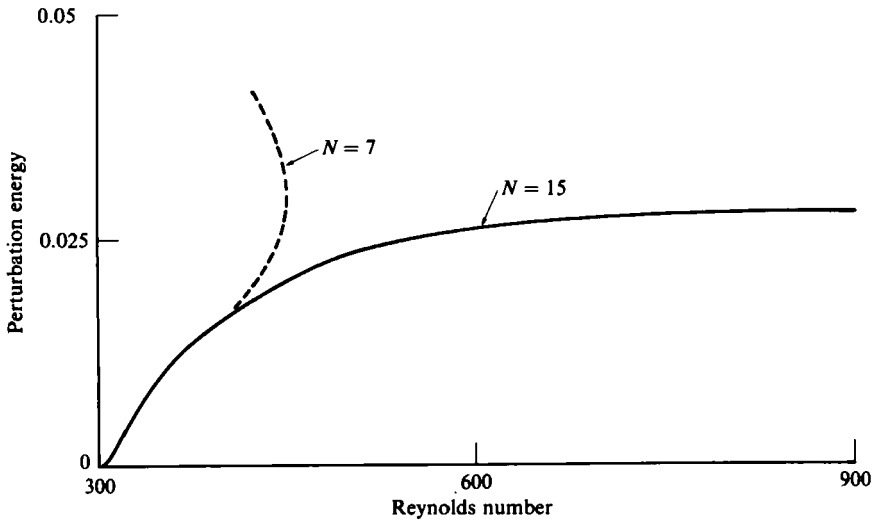
FIGURE 5. Results for unidirectional flow with Blasius profile. Energy of disturbance normalized on $\frac{1}{2}U_\infty^2 \delta_0$ versus Reynolds number $U_\infty \delta_0/\nu$. Laminar bifurcation occurs for $Re = 303$. Solid line is for $N = 15$. Dashed line shows spurious bendback with $N = 7$ caused by truncation error. $M = 99$, $y_\infty = 15$, $\alpha = 0.17$, $L = \pi\delta_0/\alpha$. $\beta = 2.5$.

side of (5.4) does not affect the number of equations, but by introducing an extra variable K, which gives the magnitude of the fictitious force, we can now impose an extra boundary condition

$$B_0 = U_\infty \tag{5.5}$$

and use this equation to determine K.

We now have a well-posed mathematical problem, and we proceed as before to calculate solutions periodic in x with wavelength L. There is a choice of parameters to vary along the solution branch. The simplest conceptually is to keep L, U_∞ and δ_0 fixed at some values and vary ν.

A Reynolds number can be defined as

$$Re = U_\infty \delta/\nu. \tag{5.6}$$

The unidirectional laminar solution that satisfies (5.4) with $K = 1$ allows bifurcation into non-uniform solutions at a value of ν given by the critical Reynolds number found from the Orr–Sommerfeld equation with the Blasius profile. The eigenfunction provides the tangent to the bifurcated branch which is followed in the usual way by continuing in ν. Some results are shown in figure 5.

The difficulty of handling the spatial growth of the boundary layer has led some investigators to consider the problem of the unsteady growing boundary layer on an infinite flat plate set into motion. When the motion is a constant velocity started impulsively from rest the velocity is referred to as the Rayleigh profile and is the unsteady one thought to correspond most closely to the Blasius profile on the semi-infinite flat plate on the basis of the analogy between t and x/U_∞. Although spatially periodic solutions can now be assumed, steady solutions do not exist and separation of variables with respect to time is not allowed. The same artifice used above can be used for the Rayleigh profile, and steady propagating solutions can be found if the laminar profile is taken to be given by

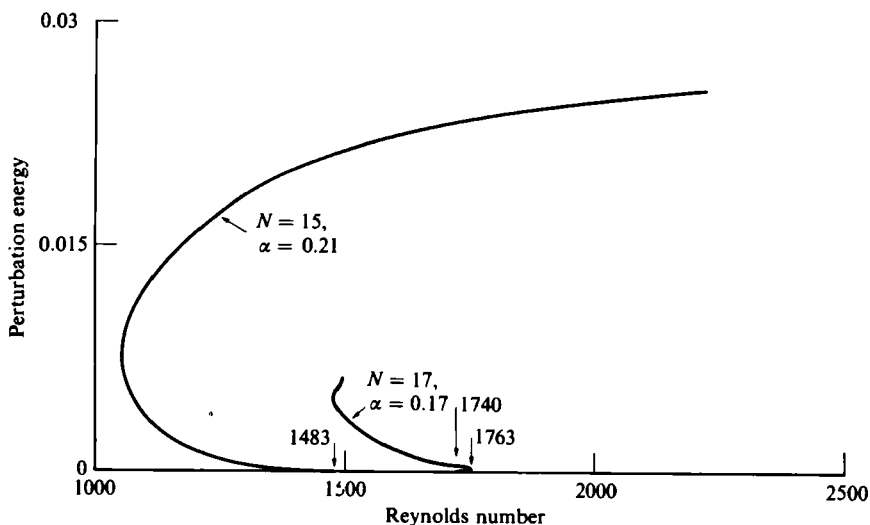$$U = U_\infty \operatorname{erfc}(y^2/\delta_0^2) \tag{5.7}$$

FIGURE 6. Results for unidirectional flow with Rayleigh profile. Normalized energy of disturbance versus Reynolds number for $\alpha = 0.17$ and 0.21. Laminar bifurcation occurs for $Re = 1740$ and 1483 respectively. $M = 149$, $y_\infty = 12.5$, $\beta = 4$. Note that for $\alpha = 0.17$ the bifurcation is initially supercritical but rapidly becomes subcritical.

with the corresponding force field. The calculation proceeds as for the Blasius layer with ν varying and L, U_∞ and δ_0 kept constant. A Reynolds number can again be defined by (5.6). Results are shown in figure 6.

It will be seen that there is a considerable difference between the Blasius profile and the Rayleigh profile. In the former case, the bifurcation is supercritical and the steady nonlinear waves corresponding to increasing x_0 or Reynolds number. (Earlier results presented by Saffman (1983) in which the curve bent back to smaller Reynolds numbers and which were made the basis of a speculation that finite-amplitude subcritical transition was possible are now found to be due to truncation error.) On the other hand, the behaviour of the Rayleigh profile depends upon the value of α. At the lowest Reynolds number for instability the bifurcation is subcritical and bends back to supercritical behaviour as the amplitude increases, as for Poiseuille flow. However, for bifurcation at larger Reynolds numbers, corresponding to a different value of α, the bifurcation is initially supercritical, but then at a very small amplitude turns back to subcritical behaviour, and then becomes supercritical again as the amplitude increases.

The main conclusion to be drawn from these results is unfortunately rather negative. It appears that there is a considerable sensitivity to the shape of the laminar profile, and that therefore results from any *ad hoc* model of the boundary layer that does not accurately take account of the growth at the Reynolds numbers for which transition occurs (and this is also the case for the so-called rational asymptotic models formally valid in the limit of $Re \to \infty$) are of doubtful significance.

6. Perturbation expansion

It is always desirable to check the accuracy of large-scale numerical calculations if possible, and in the present case some check can be performed by evaluating independently the properties of the nonlinear waves in the neighbourhood of the

bifurcation point by carrying out perturbation analysis. We let ϵ be a measure of the amplitude of the disturbance and take expansions of the form

$$\Psi(x, y) = \Psi_{00} + \epsilon(\Psi_{11}\,e^{i\alpha x} + \Psi_{11}^*\,e^{-i\alpha x})$$
$$+ \epsilon^2(\Psi_{22}\,e^{2i\alpha x} + \Psi_{00} + \Psi_{22}^*\,e^{-2i\alpha x}) + \epsilon^3(\Psi_{31}\,e^{i\alpha x} + \Psi_{31}^*\,e^{-i\alpha x}) + \dots, \quad (6.1)$$

where Ψ_{mn} is the coefficient of the nth harmonic at order m and is a function of y. In the perturbation expansion we followed the numerical approach and kept δ_0, L and U_∞ constant and varied ν. However, we now keep K constant as well and allow a perturbation in the free-stream velocity for the Blasius and Rayleigh profiles. Then, together with (6.1), we have an expansion

$$\left.\begin{aligned} c &= c_0 + \epsilon^2 c_2 + \dots, \\ \nu &= \nu_0 + \epsilon^2 \nu_0 + \dots. \end{aligned}\right\} \quad (6.2)$$

The suffix 0 refers to the values at the bifurcation point, which are given by the requirement that the Orr–Sommerfeld equation has a real eigenvalue c_0. Substitution into (5.4) and equating powers of ϵ and $\exp(i\alpha x)$ gives a set of linear inhomogeneous ordinary differential equations for the Ψ_{mn}. The linear operator is singular for $n = 1$, and the Fredholm alternative applied to the right-hand side then gives consistency conditions to determine the corrections to c and ν. In particular, the Fredholm-alternative condition applied to the equation for Ψ_{31} (that the right-hand side be orthogonal to the solution of the adjoint operator) gives one complex equation and hence two real equations, which determine c_2 and ν_2. The details are straightforward in principle and will not be described. However, we should like to emphasize that a considerable amount of work and considerable care was needed to solve the ordinary differential equations and evaluate the integrals over an infinite region with sufficient accuracy. The discretization of the y-variable and the matching to asymptotic boundary conditions was basically similar to the method described in §3 for the partial differential equation. The extra flux Q' in the boundary layer (i.e. change in displacement thickness multiplied by free-stream velocity) and extra velocity U_∞' are given by the asymptotic behaviour of Ψ_{20}:

$$\Psi \sim Q' + U_\infty' y \quad \text{as } y \to \infty. \quad (6.3)$$

Comparisons of the results obtained from the perturbation analysis and the solution of the full two-dimensional system are shown in tables 1–3 and lend support to the belief that the numerical approach is correct.

7. Conclusions

Apart from the results for the uniform suction profile, the calculations of two-dimensional steady finite-amplitude waves or vortical states in viscous shear flow reported in this paper lead unfortunately to somewhat negative conclusions about the relevance of two-dimensional calculations and the value of approximations made to handle the streamwise dependence of spatially growing flows. It appears that the three-dimensionality of real turbulent flows must be incorporated into the laminar or vortical states that are used to simulate turbulent motion if the physics is to be properly modelled. This, of course, is not a new idea, and it was perhaps unreasonably optimistic to hope that the study of two-dimensional vortical states would elucidate turbulent phenomena.

On the other hand, it appears that genuinely two-dimensional motions at large

	Perturbation theory	Numerical values	
ϵ^2	0	0.719 (-5)	0.123 (-3)
$(\nu-\nu_0)/\epsilon^2$	-0.118	-0.111	-0.109
$(c-c_0)/\epsilon^2$	4.06	4.05	4.08
Q'/ϵ^2	3.93	3.83	3.86
U'_∞/ϵ^2	6.0	5.98	6.02
E'_{22}/ϵ^2	28.0	27.90	26.8

TABLE 1. Comparison of perturbation results and numerical calculations: Blasius profile. Numerics employed: $M = 99$, $\beta = 3$, $y_\infty = 15$. For $\epsilon^2 \neq 0$, $N = 5$. $Re_0 = 303$, $\alpha = 0.17$.

	Perturbation theory	Numerical values	
ϵ^2	0	0.977 (-5)	0.763 (-3)
$(\nu-\nu_0)/\epsilon^2$	-0.064	-0.059	-0.045
$(c-c_0)/\epsilon^2$	12.8	13.0	14.0
Q'/ϵ^2	2.04	1.86	1.93
U'_∞/ϵ^2	7.95	7.94	8.15
E'_{22}/ϵ^2	174.7	173.0	160.5

TABLE 2. Comparison of perturbation results and numerical calculations: Rayleigh profile. Numerics employed $M = 149$, $\beta = 4$, $y_\infty = 12.5$. For $\epsilon^2 \neq 0$, $N = 5$. These values are for initially supercritical bifurcation at $Re_0 = 1740$, $\alpha = 0.17$.

	Perturbation theory	Numerical values
ϵ^2	0	0.183 (-4)
$(\nu-\nu_0)/\epsilon^2$	0.296	0.30
$(c-c_0)/\epsilon^2$	533	530
Q'/ϵ^2	-21.9	-21.5
E'_{22}/ϵ^2	1484	1430

TABLE 3. Comparison of perturbation results and numerical calculations: asymptotic suction profile. Numerics employed $M = 149$, $\beta = 5$, $y_\infty = 10$. For $\epsilon^2 \neq 0$, $N = 5$. $Re_0 = 54700$ for $\alpha = 0.16$.

Reynolds number may be within experimental reach (e.g. Couder, Basdevant & Thome 1984), in which case it may be possible to test the predictions made by two-dimensional calculations against experiment.

The sensitivity of the boundary-layer model to the assumed profile is discouraging, as it implies that a better understanding of the boundary conditions appropriate to spatially developing flow is needed, and at present little progress appears to have been made with this difficult problem.

REFERENCES

COUDER, Y., BASDEVANT, C. & THOME, H. 1984 Solitary vortex couples in two-dimensional wakes. *C. r. Acad. Sci., Paris* **299**, 89–93.

DRAZIN, P. G. & REID, W. H. 1981 *Hydrodynamic Stability*. Cambridge University Press.

GOLDSHTIK, M. A., LIFSHITS, A. M. & SHTERN, V. N. 1983 The transition Reynolds number for a plane channel. *Dokl. Akad. Nauk SSSR* **273**, 75–79.

HERBERT, T. 1978 Die neutrale Fläche der ebenen Poiseuille-Strömung. Habilitationsschrift, Universität Stuttgart.

HERBERT, T. 1981 Stability of plane Poiseuille flow – theory and experiment. *Fluid Dyn. Trans.* **11**, 77–126.

HOCKING, L. M. 1975 Non-linear instability of the asymptotic suction velocity profile. *Q. J. Mech. Appl. Maths* **28**, 341–353.

KELLER, H. B. 1977 Numerical solution of bifurcation and nonlinear eigenvalue problems. In *Applications of Bifurcation Theory* (ed. P. H. Rabinowitz), p. 359. Academic.

NOETHER, F. 1921 Das Turbulenzproblem. *Z. angew. Math. Mech.* **1**, 125–138, 218–219.

ORSZAG, S. A. & PATERA, A. T. 1983 Secondary instability of wall-bounded shear flows. *J. Fluid Mech.* **128**, 347–385.

ROZHDESTVENSKY, B. L. & SIMAKIN, I. N. 1984 Secondary flow in a plane channel: their relationship and comparison with turbulent flows. *J. Fluid Mech.* **147**, 261–289.

SAFFMAN, P. G. 1983 Vortices, stability and turbulence. In *Proc. 4th Intl Conf. Physico-Chemical Hydrodynamics* (ed. R. Pfeffer); *Ann. NY Acad. Sci.* **404**, 12–24.

SMITH, F. T. & BODONYI, R. J. 1982 Amplitude dependent neutral modes in the Hagen–Poiseuille flow through a circular pipe. *Proc. R. Soc. Lond.* A **384**, 463–489.